Assessment of the Sr-Mn-O System

A. Nicholas Grundy, Bengt Hallstedt, and Ludwig J. Gauckler

(Submitted November 26, 2003; in revised form May 3, 2004)

A thermodynamic assessment of the Sr-Mn-O system is presented. The main practical relevance of this system is that it contains the perovskite phase SrMnO$_3$, which is the Sr-rich end member of the phase (La,Sr)MnO$_3$, that finds widespread use as a cathode material for solid oxide fuel cells (SOFCs) and has recently attracted a lot of attention due to its interesting giant magneto-resistive properties. The thermodynamic parameters are optimized by applying the CALPHAD method. The SrMnO$_{3-z}$ phase exists in two modifications, a layered hexagonal modification at low temperatures and a perovskite modification at high temperatures. Both modifications show considerable oxygen deficiencies, which are modeled using the compound energy model. The sublattice occupation of the phases is (Sr^{2+}) (Mn^{3+}, Mn^{4+})(O^{2-}, Va)$_3$. On reducing Mn^{4+} to Mn^{3+}, oxygen vacancies are formed. The phase SrMn$_3$O$_{6-z}$ also shows an oxygen deficiency, which is modeled in an identical way. The Ruddlesden-Popper phases Sr$_2$MnO$_4$ and Sr$_3$Mn$_2$O$_7$, and the phases Sr$_7$Mn$_4$O$_{15}$ and Sr$_4$Mn$_3$O$_{10}$ are modeled as stoichiometric phases. The ionic liquid is modeled using the two-sublattice model for ionic liquids. The stability and thermodynamic data on many of the phases in this system are poorly known. For this reason, some aspects of this assessment must be regarded as tentative.

1. Introduction

Interest in La-Sr-Mn oxides stems from two fields of application for these compounds. On the one hand, (La,Sr)MnO$_3$ perovskites are well-established materials for solid oxide fuel cell (SOFC) cathodes.[1] On the other hand, both compounds crystallizing in the three-dimensional (3D) perovskite structure,[2] and, more recently, the layered compounds crystallizing in tetragonal structures, exemplified by the $n = 2$ member of the Ruddlesden-Popper series La$_{2-2x}$Sr$_{1+2x}$MnO$_7$,[3] have received much attention due to their giant (or colossal) magnetoresistive properties. In contrast to the wealth of articles published on these La-Sr-Mn-O phases, rather little is known about the phases in the Sr-Mn-O subsystem as, with the exception of the phase Sr$_7$Mn$_4$O$_{15}$, which is being considered as a high-temperature, negative temperature coefficient (NTC) thermistor,[4] no practical uses for these phases are envisaged. However, should the thermodynamic properties of the quaternary system be described properly, it is imperative that the thermodynamic properties of the lower order systems be well described. Here, an assessment of the Sr-Mn-O system is presented.

The most well-known phases in the Sr-Mn-O system are the layered hexagonal and perovskite modifications of the composition SrMnO$_{3-z}$.[5-8] Below 1730 K in air, the four-layer hexagonal phase (hereafter designated 4H-SrMnO$_{3-z}$) is stable, and above this temperature the perovskite phase (hereafter designated P-SrMnO$_{3-z}$) is stable. With decreasing oxygen partial pressure, the transition temperature is reduced. Both modifications show oxygen deficiency. The Mn in stoichiometric SrMnO$_3$ has the valency state Mn^{4+}. At high temperatures and low oxygen partial pressures, Mn^{4+} is reduced to Mn^{3+}, and the oxygen deficiency becomes more pronounced. The end-member phase on reduction has the composition SrMnO$_{2.5}$. Here all the manganese is reduced from Mn^{4+} to Mn^{3+}. This brownmillerite-like compound is often referred to as a separate phase;[7-9] however, here it is simply regarded as the end member of the P-SrMnO$_{3-z}$ phase; this view is based on some more recent investigations.[10-12] In addition to these phases of composition SrMnO$_{3-z}$, a series of phases with the general composition Sr$_{n+1}$Mn$_n$O$_{3n+1}$, with $n = 1$, 2, and 3, have been reported.[9] Two of these phases, Sr$_2$MnO$_4$ and Sr$_3$Mn$_2$O$_7$, belong to the Ruddlesden-Popper family,[13] the phase Sr$_4$Mn$_3$O$_{10}$, on the other hand, does not. The phase Sr$_2$MnO$_4$ was sometimes thought to exist in an α- and β-modification;[9,14] however, what was thought to be the α-modification was found to be the phase Sr$_7$Mn$_4$O$_{15}$ of slightly different composition, which is stable below 1823 K in air.[4,15] The phase Sr$_2$MnO$_4$ is stable above 1623 K in air. On the manganese-rich side, the phase SrMn$_3$O$_{6-z}$ is found.[6] On heating in air, this phase decomposes to β-Mn$_3$O$_4$ and 4H-SrMnO$_{3-z}$ at 1488 K. The crystal structures of these phases have been determined by a number of authors[6,9-11,16-24] and are summarized in Table 1.

In this work, thermodynamic data and information on the phase diagram from the literature are reviewed and a consistent set of thermodynamic model parameters is optimized for the system using the CALPHAD method. The thermodynamic parameters of the two border systems, Sr-O[25] and Mn-O,[26] are taken from previous optimizations. In this work, the phases 4H-SrMnO$_{3-z}$, perovskite, and SrMn$_3$O$_{6-z}$ are described using the compound-energy model[27,28] and the ionic liquid using the two-sublattice model for ionic liquids.[29,30] The Ruddlesden-Popper phases Sr$_2$MnO$_4$ and

A. Nicholas Grundy and **Ludwig J. Gauckler,** ETH Zurich, Department of Materials, Institute of Nonmetallic Materials, Swiss Federal Institute of Technology, CH-8092 Zurich, Switzerland; and **Bengt Hallstedt,** RWTH Aachen, Materials Chemistry, D-52074 Aachen, Germany. Contact e-mail: grundy@mat.ethz.ch.

Table 1 Crystal Structures of the Phases Reported in the Sr-Mn-O System

Name	Composition	Space Group	Structure Type	References
Brownmillerite	$SrMnO_{2.5}$	*Pbam* or *Pba2 Pbam*	$Ca(Al,Fe)O_{2.5}$	Caignaert et al.[10] Mori et al.[11]
4H-SrMnO$_{3-z}$	$SrMnO_{3-z}$	*P6$_3$/mmc*	$BaMnO_3$	Kuroda et al.[16] Battle et al.[17]
Perovskite	$SrMnO_{3-z}$	*Pnma*	$GdFeO_3$	Tichy and Goodenough[18]
2:1 Ruddlesden-Popper Phase	Sr_2MnO_4	*R$\bar{3}$c I4/mmm*	K_2NiF_4	Balz and Plieth[19] Tezuka et al.[20]
Layered 3:2 Ruddlesden-Popper Phase	$Sr_3Mn_2O_7$	*I4/mmm*	$Sr_3Ti_2O_7$	Mizutani et al.[9] Mitchell et al.[21]
4:3 Phase	$Sr_4Mn_3O_{10}$	*Cmca*	$Sr_4Ti_3O_{10}$	Fabry et al.[22] Floros et al.[23]
$Sr_7Mn_4O_{15}$	$Sr_7Mn_4O_{15}$	*P2$_1$/c*	...	Vente et al.[24]
$SrMn_3O_{6-z}$	$SrMn_3O_{6-z}$	Orthorhombic	...	Negas[6]

$Sr_3Mn_2O_7$ and the phases $Sr_4Mn_3O_{10}$ and $Sr_7Mn_4O_{15}$ are described as stoichiometric compounds, as there are no experimental data on oxygen deficiency, although it is very likely that these phases are also oxygen-deficient.

2. Literature Survey

2.1 Phase Diagram

Mizutani et al.[9] investigated the stability of the phases $Sr_{n+1}Mn_nO_{3n+1}$. According to their work, the phase Sr_2MnO_4 exists in an α-modification up to 1673 K, and in a β-modification at 1773 K and above. The β-modification corresponds to the $n = 1$ Ruddlesden-Popper phase, belonging to the space group *I4/mmm*.[19,31] Tezuka et al.[20] prepared the β-modification in oxygen at 1923 K and confirmed the crystal structure that had previously been determined. Measurements of the electrical conductivity of β-Sr_2MnO_4 prepared in oxygen at 1923 K by Bouloux et al.[31] revealed low conductivities and high activation energy for conduction, suggesting the presence of relatively few Mn^{3+}, and consequently a relatively low degree of reduction and a small number of oxygen vacancies. The XRD pattern ascribed to the phase α-Sr_2MnO_4 was later shown by Kriegel et al.[15] and Feltz et al.[4] to belong to a mixture of the phases SrO and $Sr_7Mn_4O_{15}$. The phase $Sr_7Mn_4O_{15}$ has additionally been synthesized and characterized by Vente and colleagues.[24,32] The phase α-Sr_2MnO_4, therefore, does not exist. Kriegel et al.[15] and Feltz et al.[4] determined the decomposition temperature of β-Sr_2MnO_4 into SrO and $SrMn_4O_{15}$ to be around 1623 K in air. The phase $Sr_3Mn_2O_7$ does not form up to 1873 K, but is stable at 1973 and 2073 K.[9] The decomposition is thus assumed to take place at 1923 K. Mitchell et al.[21] synthesized this phase at 1923 K in air and determined it to be the tetragonal $n = 2$ Ruddlesden-Popper phase with space group *I4/mmm.* Their phase showed considerable oxygen deficiency and was analyzed to have the composition $Sr_3Mn_2O_{6.55}$. Annealing the sample in oxygen at 673 K almost completely oxidized the sample to the composition $Sr_3Mn_2O_{6.98}$. The phase

$Sr_4Mn_3O_{10}$, which crystallizes in the space group *Cmca*[22,23] and is not a Ruddlesden-Popper phase, is only stable at 1673 and 1773 K, and decomposes at both higher and lower temperatures according to Mizusaki et al.[9] Floros et al.,[23] on the other hand, were able to synthesize the phase in evacuated silica tubes at 1373 K, and Fabry et al.[22] grew crystals, albeit with small impurities of platinum in their crystal structure, from melts based on $SrCl_2$-SrF_2-B_2O_3 in platinum crucibles at temperatures around 1473 K. The result of the work of Mizutani et al.[9] that the phase $Sr_4Mn_3O_{10}$ is metastable at 1573 K and below must therefore be regarded as questionable. In addition, Bochu et al.[33] synthesized the phase $SrMn_7O_{12}$ at 50 kbar and 1273 K. This phase is most likely metastable at ambient conditions and was not considered in this work.

To summarize, four phases are stable in air in the SrO-rich half of the SrO-MnO_x portion of the Sr-Mn-O system. Two phases are stable at low temperatures, $Sr_7Mn_4O_{15}$ and $Sr_4Mn_3O_{10}$; both decompose on heating above 1823 and 1773 K, respectively. The two Ruddlesden-Popper phases, Sr_2MnO_4 and $Sr_3Mn_2O_7$, are stable at high temperatures and decompose on cooling below 1873 and 1923 K, respectively. The phase, hitherto described as α-Sr_2MnO_4, is now known to have the slightly different composition of $Sr_7Mn_4O_{15}$.

The first determination of oxygen deficiency in $SrMnO_{3-z}$ was conducted by Jonker and van Santen[34] in air at 1623 K. A systematic investigation of the phase $SrMnO_{3-z}$ was later conducted by Negas and Roth[5] and Negas.[6] They measured the oxygen deficiency in air as a function of temperature. They found that below 1673 K the four-layer hexagonal $SrMnO_{3-z}$ is stable, and that above 1673 K the perovskite phase is stable. The transition in air on heating is accompanied by a reduction of the oxygen content from $SrMnO_{2.89}$ to $SrMnO_{2.74}$. They further determined the melting temperature of the perovskite phase to be 2013 K in air[5] and the temperature of the three-phase equilibrium β-Mn_3O_4 + $SrMnO_{3-z}$ + liquid in air to be 1688 K.[6] In a more complete study, Kuroda et al.[7,8] measured the oxygen deficiency of $SrMnO_{3-z}$ as a function of tem-

perature for oxygen partial pressures ranging from 10^{-6} to 1 bar. At low oxygen partial pressures and high temperatures, they found what they described as a brownmillerite-like phase, $SrMnO_{2.5+x}$. Chmaissem et al.,[12] on the other hand, determined a composition of $SrMnO_{2.61}$ and the perovskite structure for their sample annealed in 10 ppm O_2 at 1673 K. Caignaert et al.[10] reduced $SrMnO_{3-z}$ in the presence of zirconium at 773 K in silica ampoules and obtained a phase of composition $SrMnO_{2.5}$ with an orthorhombic crystal structure belonging to the space group *Pbam* or *Pba2*. They found that the phase does not belong to the brownmillerite family, as claimed by Mizutani et al.,[9] but is closely related to the perovskite $SrMnO_3$. Mori et al.[11] synthesized a phase with a composition close to $SrMnO_{2.5}$ by annealing $SrMnO_3$ in 0.1% H_2 + Ar at 1373 K. They assigned the phase to the space group *Pbam*, thereby confirming the findings of Caignaert et al.[10] The crystal structure of $SrMnO_3$ was determined by Kuroda et al.[16] to belong to the space group $P6_3/mmc$. This was later confirmed by Battle et al.[17] using neutron diffraction. Tichy and Good-enough[18] determined the crystal structure of the perovskite phase to be of the $GdFeO_3$ structure type, belonging to the *Pbnm* or *Pnma* space group.

The manganese-rich portion of the pseudobinary SrO-MnO_x section through the Sr-Mn-O system in air was investigated by Negas.[6] He found that the phase $SrMn_3O_{6-z}$ decomposes at 1488 K. He also determined the oxygen deficiency of $SrMn_3O_{6-z}$ as a function of temperature.

2.2 Thermodynamic Data

The enthalpies of formation, $\Delta_f^o H_{298}$, and the entropies of the phases in the Sr-Mn-O system have been assessed by Yokokawa et al.[35] who used estimations of stabilization energies using the Goldschmidt tolerance factors for the various structures. Rørmark et al.[36] measured the enthalpy of formation of $SrMnO_{2.946}$ using drop calorimetry.

The partial Gibbs energy for the reaction $SrMnO_{2.5} \rightarrow$ SrO + MnO + 1/2O_2 has been determined by Tanasescu et al.[37] by emf measurements using the equilibrium Fe/Fe_xO as reference. What Tanasescu et al.[37] described as a brownmillerite-like compound, is interpreted to be a strongly reduced perovskite based on recent structural data.[10-12]

3. Thermodynamic Modeling

3.1 The Ionic Liquid

The two-sublattice model for ionic liquids,[29,30] herein used to describe the liquid phase, was developed for liquids that show ionic behavior of the components. The model follows the work of Temkin[38] and assumes that the anions and cations occupy separate sublattices and are allowed to mix freely on their respective sublattices. Hypothetical vacancies are introduced on the anion sublattice to maintain charge neutrality and to allow a description toward a metallic liquid containing cations only.

In the Sr-Mn-O system the model is represented as

$$(Sr^{2+}, Mn^{2+}, Mn^{3+})_p(O^{2-}, Va^{q-})_q \qquad \text{(Eq 1)}$$
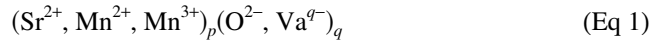
The number of sites on the respective sublattices p and q must vary with composition to maintain charge neutrality. Mn^{4+} is not included, as Mn^{4+} is not known to exist in the liquid at ambient oxygen partial pressures. The values of p and q are calculated by

$$p = 2y_{O^{2-}} + qy_{Va^{q-}} \qquad \text{(Eq 2)}$$

$$q = 2y_{Sr^{2+}} + 3y_{Mn^{3+}} + 2y_{Mn^{2+}} \qquad \text{(Eq 3)}$$

where y represents the site fraction of a particular species on the respective sublattice. The hypothetical vacancies have an induced charge of $-q$.

The molar Gibbs energy of the liquid is given by

$$G_m^{Liq} = \sum_{i=cations} y_i y_{O^{2-}} \cdot {}^o G_{i:O^{2-}}^{Liq} + q \sum_{i=cations} y_i y_{Va^{q-}} \cdot {}^o G_{i:Va^{q-}}^{Liq}$$
$$+ RT \cdot \left(p \sum_{i=cations} y_i \ln y_i + q \sum_{j=anions} y_j \ln y_j \right) + {}^E G_m^{Liq}$$
$$\text{(Eq 4)}$$

The Gibbs energies of liquid Sr and Mn, ${}^o G_{Sr^{2+}:Va^{q-}}^{Liq}$ and ${}^o G_{Mn^{2+}:Va^{q-}}^{Liq}$, respectively, are taken from Dinsdale,[39] and the Gibbs energies of the oxides, ${}^o G_{Mn^{2+}:O^{2-}}^{Liq}$, ${}^o G_{Mn^{3+}:O^{2-}}^{Liq}$, and ${}^o G_{Sr^{2+}:O^{2-}}^{Liq}$ are taken from previous assessments of the Mn-O[26] and Sr-O[25] systems.

The excess Gibbs energy ${}^E G_m^{Liq}$ is given by

$$^E G_m^{Liq} = \sum {}^E G_{binaries}^{Liq} + \sum {}^E G_{ternaries}^{Liq} \qquad \text{(Eq 5)}$$

where $\sum {}^E G_{binaries}^{Liq}$ is taken from the binaries and $\sum {}^E G_{ternaries}^{Liq}$ represents the ternary interaction parameters. In this work, the ternary interaction parameters ${}^0 L_{Sr^{2+}, Mn^{2+}:O^{2-}}^{Liq}$ and ${}^0 L_{Sr^{2+}, Mn^{3+}:O^{2-}}^{Liq}$ were optimized.

3.2 The Perovskite and Four-Layered Hexagonal Modifications of SrMnO₃₋ᵤ

Both the four-layer hexagonal and the perovskite phases of the composition $SrMnO_{3-z}$ show considerable oxygen deficiency, which increases with increasing temperature or reducing oxygen partial pressure. The end member on reduction has the composition $SrMnO_{2.5}$. This compound was originally sometimes described as a separate brownmillerite-like phase.[7,8] Later, however, it was shown not to have the brownmillerite structure, but a structure very closely resembling the structure of the perovskite phase.[10-12] For this reason, the phase $SrMnO_{2.5}$ is described not as a separate phase, but as the reduced end point of the perovskite phase. The sublattice occupation for both the 4H-$SrMnO_{3-z}$ and P-$SrMO_{3-z}$ phases is given as

$$(Sr^{2+})_1(Mn^{3+}, Mn^{4+})_1(O^{2-}, Va)_3 \qquad \text{(Eq 6)}$$
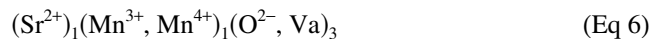
In the compound energy formalism,[27,28] this gives four end-member compounds, $(Sr^{2+})(Mn^{3+})(O^{2-})_3$, (Sr^{2+})

$(Mn^{3+})(Va^-)_3$, $(Sr^{2+})(Mn^{4+})(O^{2-})_3$, and $(Sr^{2+})(Mn^{4+})(Va)_3$, that need to be given Gibbs energies. The Gibbs energy of the perovskite or four-layered hexagonal phase of arbitrary composition, including entropy and excess Gibbs energy, is given as

$$^oG_m = y_{Sr^{2+}}y_{Mn^{4+}}y_{O^{2-}}{}^oG_{Sr^{2+}:Mn^{4+}:O^{2-}} + y_{Sr^{2+}}y_{Mn^{4+}}y_{Va}{}^oG_{Sr^{2+}:Mn^{4+}:Va}$$
$$+ y_{Sr^{2+}}y_{Mn^{3+}}y_{O^{2-}}{}^oG_{Sr^{2+}:Mn^{3+}:O^{2-}}$$
$$+ y_{Sr^{2+}}y_{Mn^{3+}}y_{Va}{}^oG_{Sr^{2+}:Mn^{3+}:Va} + RT[(y_{Mn^{4+}}\ln y_{Mn^{4+}}$$
$$+ y_{Mn^{3+}}\ln y_{Mn^{3+}}) + 3(y_{O^{2-}}\ln y_{O^{2-}} + y_{Va}\ln y_{Va})] + {}^EG_m^{Perov}$$

$$\text{(Eq 7)}$$

The term $^EG_m^{Perov}$ represents the excess Gibbs energy. What needs to be done now is to assign values to the four ^oG parameters. Giving the four parameter values directly is impractical, as three of the four ^oG parameters describe compounds with a net charge that can therefore not physically exist. Therefore, what needs to be done is to express the four ^oG parameters using the Gibbs energies of the neutral compounds $(Sr^{2+})(Mn^{4+})(O^{2-})_3$ and $(Sr^{2+})(Mn^{3+})$ $(5/6\ O^{2-},\ 1/6\ Va)_3$, which form the two end points of the solid solution and are experimentally accessible. In the following discussion, the Gibbs energies of these two neutral end members will be denoted by $GS4O$ and $GS3O$, respectively. These two neutral end points can be given as

$$GS4O = {}^oG_{Sr^{2+}:Mn^{4+}:O^{2-}} \qquad \text{(Eq 8)}$$

and

$$GS3O = \frac{5}{6}{}^oG_{Sr^{2+}:Mn^{3+}:O^{2-}} + \frac{1}{6}{}^oG_{Sr^{2+}:Mn^{3+}:Va}$$
$$+ 3RT\left(\frac{5}{6}\ln\frac{5}{6} + \frac{1}{6}\ln\frac{1}{6}\right) \qquad \text{(Eq 9)}$$

where the last term in Eq 9 is the configurational entropy of the reduced phase. Two further equations are needed to define all four ^oG parameters. The first one is given by a reference point, which is defined as follows

$$^oG_{Sr^{2+}:Mn^{4+}:Va} = GS4O - \frac{3}{2}{}^oG_{O_2}^{Gas} \qquad \text{(Eq 10)}$$

The last equation results from regarding the four ^oG parameters as a reciprocal system, with the Gibbs energy of the reciprocal reaction:

$$\Delta G_R = {}^oG_{Sr^{2+}:Mn^{4+}:O^{2-}}^{Perov} + {}^oG_{Sr^{2+}:Mn^{3+}:Va}^{Perov,\ 4\text{-}H} - {}^oG_{Sr^{2+}:Mn^{4+}:Va}^{Perov}$$
$$- {}^oG_{Sr^{2+}:Mn^{3+}:O^{2-}}^{Perov,\ 4\text{-}H} \qquad \text{(Eq 11)}$$

Solving Eq 8-11 for the four unknown ^oG values leads to the following result:

$$^oG_{Sr^{2+}:Mn^{4+}:O^{2-}}^{Perov} = GS4O \qquad \text{(Eq 12)}$$

$$^oG_{Sr^{2+}:Mn^{4+}:Va}^{Perov} = GS4O - \frac{3}{2}{}^oG_{O_2}^{Gas} \qquad \text{(Eq 13)}$$

$$^oG_{Sr^{2+}:Mn^{3+}:O^{2-}}^{Perov,\ 4\text{-}H} = GS3O + \frac{1}{4}{}^oG_{O_2}^{Gas}$$

$$- 3RT\left[\frac{5}{6}\ln\left(\frac{5}{6}\right) + \frac{1}{6}\ln\left(\frac{1}{6}\right)\right] - \frac{1}{6}\Delta G_R$$

$$\text{(Eq 14)}$$

$$^oG_{Sr^{2+}:Mn^{3+}:Va}^{Perov,\ 4\text{-}H} = GS3O - \frac{5}{4}{}^oG_{O_2}^{Gas}$$

$$- 3RT\left[\frac{5}{6}\ln\left(\frac{5}{6}\right) + \frac{1}{6}\ln\left(\frac{1}{6}\right)\right] + \frac{5}{6}\Delta G_R$$

$$\text{(Eq 15)}$$

This manipulation results in only two parameters, $GS4O$ and $GS3O$, representing the stoichiometric perovskite, or 4H, phase and the completely reduced perovskite, or 4H, phase, respectively, that can be optimized. The Gibbs energy of the reciprocal reaction ΔG_R is an additional parameter that could also be optimized.

3.3 The Phase SrMn$_3$O$_{6-z}$

There exists one series of measurements on oxygen deficiency in air as a function of temperature in the phase $SrMn_3O_{6-z}$.[5] The following sublattice occupancy is chosen for this phase:

$$(Sr^{2+})_1(Mn^{3+})_2(O^{2-})_3(Mn^{3+}, Mn^{4+})_1(O^{2-}, Va)_3 \qquad \text{(Eq 16)}$$

By choosing this sublattice occupation, the oxygen deficiency in this phase can be modeled in an analogous way to the perovskite and 4H phases. The parameters that then need to be optimized are $^oG_{SrMn_3O_6}$ for the stoichiometric phase and $^oG_{SrMn_3O_{5.5}}$ for the reduced phase corresponding to the parameters $GS4O$ and $GS3O$, respectively, for the perovskite and 4H phases.

3.4 The Phases Sr$_2$MnO$_4$, Sr$_3$Mn$_2$O$_7$, Sr$_4$Mn$_3$O$_{10}$, and Sr$_7$Mn$_4$O$_{15}$

Despite the interesting magnetic and other properties of these phases when doped with lanthanum, very little is known about their thermodynamics and stability. All the phases probably show oxygen deficiency due to their similarity to the perovskite and 4H phases. However, no measurements exist in the literature that could be used for an optimization of their oxygen nonstoichiometry. These phases are therefore modeled as stoichiometric phases.

4. Optimization of Parameters

The thermodynamic parameters were optimized using the PARROT module of the Thermo-Calc[40] database sys-

tem by minimizing the sum of squared errors between selected and weighted experimentally determined thermodynamic and phase diagram data from the literature and the corresponding calculated data.

4.1 The Perovskite and Four-Layered Hexagonal Modifications of SrMnO$_{3-z}$

The only measurements of the thermodynamic properties of these phases are emf measurements of the com-

Table 2 Thermodynamic Parameters for the Sr-Mn-O System

4H-SrMnO$_{3-z}$:(Sr^{2+})(Mn^{3+}, Mn^{4+})(O^{2-}, Va)$_3$
$^oG^{4H}_{SrMnO_3} = G_{SrO} + G_{MnO_2} - 111\,300$
$^oG^{4H}_{SrMnO_{2.5}} = G_{SrO} + \frac{1}{2}G_{Mn_2O_2} - 7730 - 17T$
Perovskite-SrMnO$_{3-z}$: (Sr^{2+})(Mn^{3+}, Mn^{4+})(O^{2-}, Va)$_3$
$^oG^{Perov}_{SrMnO_3} = {}^oG^{4H}_{SrMnO_3} + 22\,650 - 7.69T$
$^oG^{Perov}_{SrMnO_{2.5}} = {}^oG^{4H}_{SrMnO_{2.5}} - 14\,455$
SrMn$_3$O$_{6-z}$: (Sr^{2+})(Mn^{3+})$_2$(O^{2-})$_3$(Mn^{3+}, Mn^{4+})(O^{2-}, Va)$_3$
$^oG^{SrMn_3O_{6-z}}_{SrMn_3O_6} = {}^oG^{4H}_{SrMnO_3} + G_{Mn_2O_3} - 8791$
$^oG^{SrMn_3O_{6-z}}_{SrMn_3O_{5.5}} = {}^oG^{4H}_{SrMnO_{2.5}} + G_{Mn_2O_3} - 21\,920$
Sr$_2$MnO$_4$
$^oG_{Sr_2MnO_4} = G_{MnO_2} + 2G_{SrO} - 132\,830$
Sr$_7$Mn$_4$O$_{15}$
$^oG_{Sr_7Mn_4O_{15}} = 4G_{MnO_2} + 7G_{SrO} - 612\,450 + 50T$
Sr$_3$Mn$_2$O$_7$
$^oG_{Sr_3Mn_2O_7} = 2G_{MnO_2} + 3G_{SrO} - 89\,910 - 90T$
Sr$_4$Mn$_3$O$_{10}$
$^oG_{Sr_4Mn_3O_{10}} = 3G_{MnO_2} + 4G_{SrO} - 378\,500$
Ionic liquid: (Sr^{2+}, Mn^{2+}, Mn^{3+})p(O^{2-}, Va^{-q})$_q$
$^0L_{Mn^{2+},\ Sr^{2+}:O^{2-}} = -176\,300,\ ^0L_{Mn^{3+},\ Sr^{2+}:O^{2-}} = -176\,300$
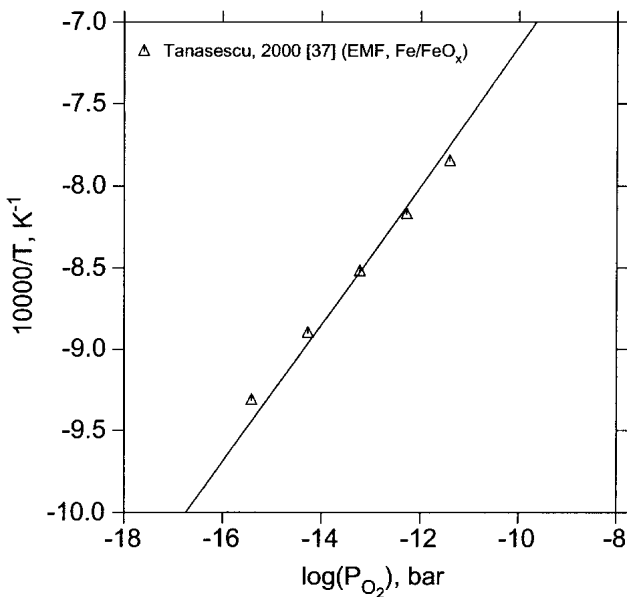
pletely reduced perovskite phase with the composition SrMnO$_{2.5}$.[37] These data fix the parameter $^oG^{Perov}_{SrMnO_{2.5}}$ for the reduced end point of the perovskite. The parameters $^oG^{Perov}_{SrMnO_3}$, $^oG^{4\text{-}H}_{SrMnO_{2.5}}$, and $^oG^{4\text{-}H}_{SrMnO_3}$ are optimized mainly with the data on oxygen deficiency as a function of oxygen partial pressure and temperature measured by Negas and Roth[5] and by Kuroda et al.,[7] and the temperature of the transition from the 4H to the perovskite phase as a function of oxygen partial pressure was also measured by Kuroda et al.[7] The estimates of the enthalpies of formation by Yokokawa et al.[35] and the measured enthalpy of formation of 4H-SrMnO$_3$ by Rørmark et al.[36] also were used for the optimization; however, they were given only a small weight due to their large uncertainty. The values of the optimized parameters are given in Table 2.

4.2 The Phase SrMn$_3$O$_{6-z}$

The temperature of decomposition at 1488 K in air and some data on oxygen nonstoichiometry in air measured by Negas and Roth[5] are the only data known about this phase. The parameters $^oG_{SrMn_3O_6}$ and $^oG_{SrMn_3O_{5.5}}$ were optimized without any temperature dependence. Their values are listed in Table 2.

4.3 The Phases Sr$_2$MnO$_4$, Sr$_3$Mn$_2$O$_7$, Sr$_4$Mn$_3$O$_{10}$, and Sr$_7$Mn$_4$O$_{15}$

The only thing that is known about these phases is their approximate temperature range of stability in air. No data exist on their thermodynamic properties, apart from estimated enthalpies of formation of Sr$_2$MnO$_4$ and Sr$_3$Mn$_2$O$_7$, which were determined by Yokokawa et al.[35] This of course makes the optimization very uncertain. It was not possible to optimize $A + BT$ terms for all phases. No temperature-dependent term was optimized for the phases Sr$_2$MnO$_4$ and Sr$_4$Mn$_3$O$_{10}$, and the phases Sr$_7$Mn$_4$O$_{15}$ and Sr$_3$Mn$_2$O$_7$ were given fixed temperature dependencies of

Fig. 1 Experimentally determined Gibbs energy for the reaction P-SrMnO$_3$→SrO + MnO + 1/2O$_2$(g) displayed as dissociation pressure as a function of inverse temperature
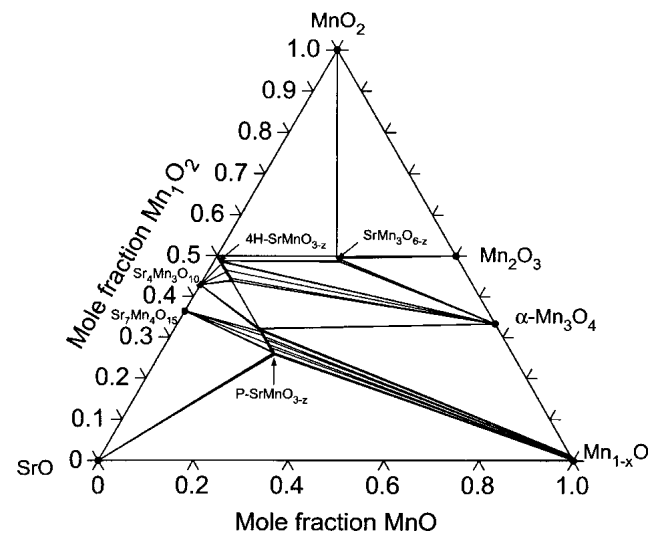

Fig. 2 Calculated isothermal section at 1273 K through the Sr-Mn-O system
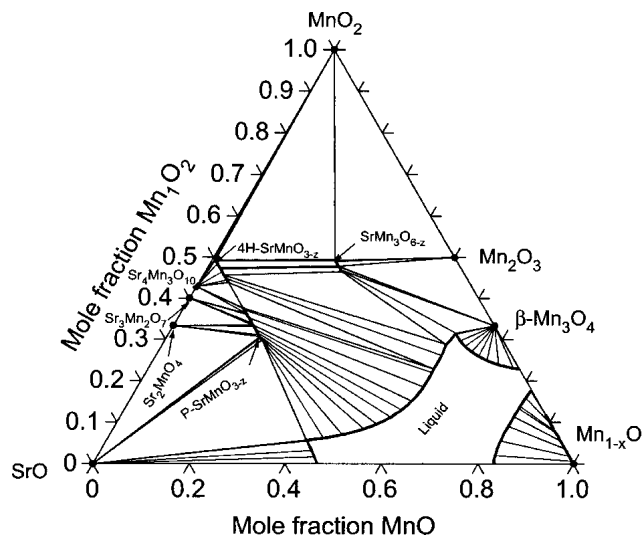
Fig. 3 Calculated isothermal section at 1873 K through the Sr-Mn-O system
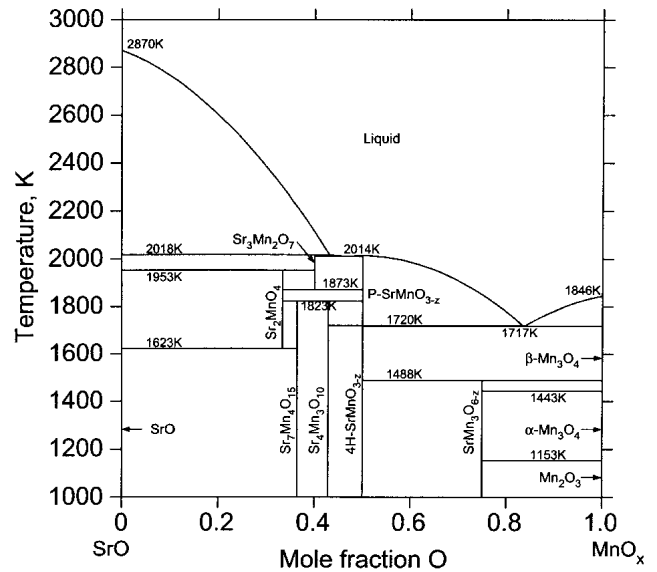

Fig. 4 Calculated SrO-MnO$_x$ phase diagram in air

Table 3 Measured and Estimated Heat of Formation $\Delta_f^o H_{298}$ From the Elements and $\Delta_f^o H_{298}$ From the Oxides of the Phases in the Sr-Mn-O System Compared to the Calculated Values

Phase	Method	$\Delta_f^o H_{298}$ From the Elements, kJ/mol	$\Delta_f^o H_{298}$ From the Oxides, kJ/mol	S_{298}, J/mol · K	References
4H-SrMnO$_3$	Estimated	−1258.5	−145.87	107.5	Yokokawa et al.[35]
	Drop calorimetry	−1201.2	−88.57	…	Rørmark et al.[36]
	Assessed	−1223.9	−111.27	107.6	This work
Perovskite SrMnO$_3$	Estimated	−1233.03	−120.4	117.5	Yokokawa et al.[35]
	Assessed	−1201.3	−88.67	115.2	This work
4H-SrMnO$_{2.5}$	Estimated	−1169.0	−95.56	95.0	Yokokawa et al.[35]
	Assessed	−1081.2	−7.75	126.7	This work
Perovskite SrMnO$_{2.5}$	Estimated	−1158.03	−84.59	110.0	Yokokawa et al.[35]
	Assessed	−1095.6	−22.15	126.7	This work
SrMn$_3$O$_6$	Estimated	−2208.3	−133.08	231.5	Yokokawa et al.[35]
	Assessed	−2195.3	−120.08	219.7	This work
Sr$_2$MnO$_4$	Estimated	−1868.0	−163.22	171.85	Yokokawa et al.[35]
	Assessed	−1837.6	−132.82	161.2	This work
Sr$_7$Mn$_4$O$_{15}$	Assessed	−6839.3	−612.33	541.0	This work
Sr$_3$Mn$_2$O$_7$	Estimated	−3111.0	−293.59	289.35	Yokokawa et al.[35]
	Assessed	−2907.3	−89.89	358.7	This work
Sr$_4$Mn$_3$O$_{10}$	Estimated	−4351.0	−420.96	418.0	Yokokawa et al[35]
	Assessed	−4308.5	−378.46	376.3	This work

Note: The heats of formation of the oxides Mn$_2$O$_3$, MnO$_2$, and SrO are taken from the assessments of the Mn-O[26] and Sr-O[25] systems, respectively.

+50 J/(mol · K) and −90 J/(mol · K), respectively. The optimized parameters are listed in Table 2.

4.4 The Ionic Liquid

The only information concerning the liquid phase is the measured melting temperature of the perovskite phase[5] and the measured temperature of the perovskite-β-Mn$_3$O$_4$-liquid equilibrium.[6] With these data, the interaction pa-

rameters $L^{Liq}_{Sr^{2+},Mn^{3+}:O^{2-}}$ and $^0L^{Liq}_{Sr^{2+},Mn^{2+}:O^{2-}}$ were optimized. They were given identical values. Their value is given in Table 2.

5. Results and Discussion

The optimized thermodynamic parameters describing the Sr-Mn-O system are listed in Table 2.
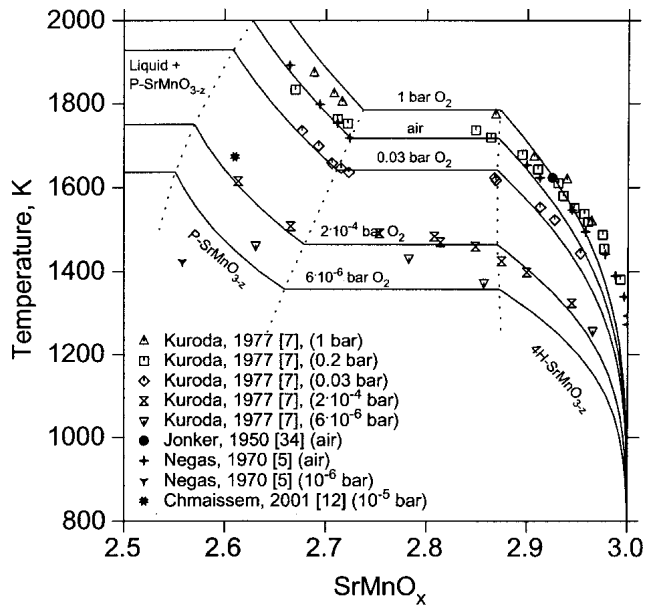
Fig. 5 Calculated oxygen content as a function of temperature and oxygen partial pressure for 4H-SrMnO$_{3-z}$ and the SrMnO$_{3-z}$ perovskite compared to experimental data from the literature
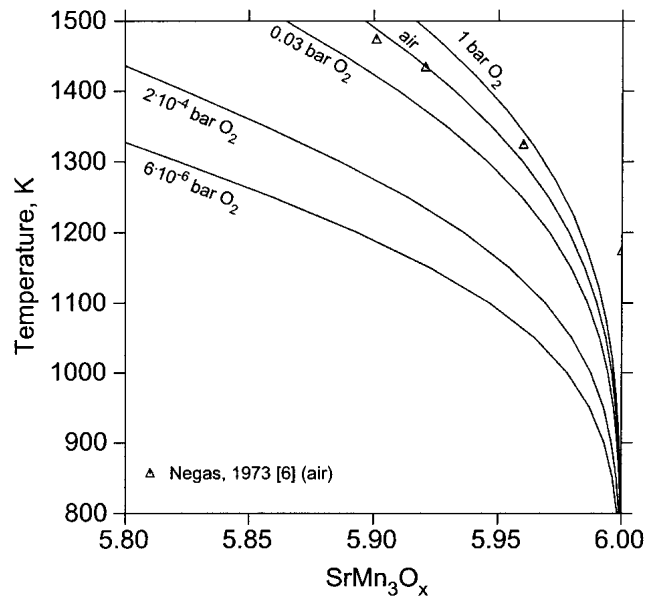
Fig. 6 Calculated oxygen content as a function of temperature and oxygen partial pressure for the phase SrMn$_3$O$_{6-z}$ compared to experimental data taken from the literature

Table 4 Calculated Temperatures of Three-Phase Equilibria, Polymorphic Transitions, and Melting Temperatures in Air, Compared to Experimental Data From Literature

Equilibrium	Calculated Temperature in Air, K	Experimentally Determined Temperature in Air(a), K	References
SrO + Sr$_7$Mn$_4$O$_{15}$ + Sr$_2$MnO$_4$	1623	1623 ± 50	Mizutani et al.[9]
P-SrMnO$_{3-z}$ + Sr$_7$Mn$_4$O$_{15}$ + Sr$_2$MnO$_4$	1823	1823 ± 50	Mizutani et al.[9]
P-SrMnO$_{3-z}$ + Sr$_3$Mn$_2$O$_7$ + Sr$_2$MnO$_4$	1873	1873 ± 50	Mizutani et al.[9]
SrO + Sr$_2$MnO$_4$ + Sr$_3$Mn$_2$O$_7$	1953	NA(b)	…
P-SrMnO$_{3-z}$ + Sr$_7$Mn$_4$O$_{15}$ + Sr$_4$Mn$_3$O$_{10}$	1823	1823 ± 50	Mizutani et al.[9]
4H-SrMnO$_{3-z}$ + SrMn$_3$O$_{6-z}$ + β-Mn$_3$O$_4$	1488	1488	Mizutani et al.[9]
4H-SrMnO$_{3-z}$ + Liquid + β-Mn$_3$O$_4$	1717	1688	Negas[6]
SrO + Sr$_3$Mn$_2$O$_7$ + Liquid	2018	NA	…
P-SrMnO$_{3-z}$ + Liquid + Sr$_3$Mn$_2$O$_7$	2011	NA	…
4H-SrMnO$_{3-z}$ → P-SrMnO$_{3-z}$	1720	1728	Kuroda et al.[7]
P-SrMnO$_{3-z}$ → Liquid	2014	2013	Negas and Roth[5] Negas[6]

(a) Values given as mean ± SD
(b) NA, not available

5.1 Thermodynamic Data

The calculated heats of formation $\Delta^o H_f$ and the entropies of the phases in the Sr-Mn-O system are compared with the values estimated by Yokokawa et al.[35] and the measurement by Rørmark et al.[36] in Table 3. It was not possible to achieve a better reproduction of the estimations by Yokokawa et al.[35] while simultaneously maintaining a reasonable fit of the phase diagram data. As the estimations of Yokokawa et al.[35] are purely empirical and deviate significantly from the only experimental value, the measure-ment on hexagonal-SrMnO$_3$, little weight was placed on these data during the optimization. The calculated Gibbs energy, which was recalculated as log(P_{O_2}) of the reaction SrO + MnO + 1/2 O$_2$ = SrMnO$_3$, is plotted as a function of the inverse temperature in Fig. 1 and is compared with the experimental data from Tanasescu et al.[37] All the measured and estimated thermodynamic data on all phases can be well reproduced by this optimization. The thermodynamic properties of phases for which no data exist are at least reasonable.

5.2 The Phase Diagram

Isothermal sections through the Sr-Mn-O system are shown in Fig. 2 and 3. Figure 4 shows the SrO-MnO$_x$ phase diagram in air. The calculated temperatures of all three-phase equilibria in air are listed in Table 4 and are compared with data from the literature. The oxygen contents of 4H-SrMnO$_{3-z}$ and P-SrMnO$_{3-z}$ are plotted as a function of temperature for various oxygen partial pressures and are compared with literature data in Fig. 5. Finally, Figure 6 shows the corresponding data for the phase SrMn$_3$O$_{6-z}$. The simple model description and the few parameters used to describe the oxygen deficiency proved to be adequate to give quite a good reproduction of the experimental data.

6. Conclusions

A rather tentative thermodynamic description of the Sr-Mn-O system using the CALPHAD approach is presented. The phases Sr$_2$MnO$_4$ and Sr$_3$Mn$_2$O$_7$, belonging to the Ruddlesden-Popper family, and the phases Sr$_4$Mn$_3$O$_{10}$ and Sr$_7$Mn$_4$O$_{15}$ are described as stoichiometric phases. As very little is known about these phases, the uncertainties about both their thermodynamic properties and ranges of stability must be considered to be quite large. The oxygen nonstoichiometry is modeled using the compound energy model[27,28] for the perovskite and layered hexagonal forms of SrMnO$_{3-z}$ and for the phase SrMn$_3$O$_{6-z}$. The liquid phase is modeled using the two-sublattice model for ionic liquids.[29,30] Despite the huge interest in the properties and the many potential uses for the above-mentioned phases doped with lanthanum, very little is known about the thermodynamics and even the phase diagram of the undoped phases. The difficulty in this case is therefore not to reproduce all experimental data correctly, but to make reasonable estimates on all the data that are missing.

References

1. N.Q. Minh and T. Takahashi: *Science and Technology of Ceramic Fuel Cells,* Elsevier Science B.V., Amsterdam, The Netherlands, 1995.
2. Y. Tokura and Y. Tomioka: "Colossal Magnetoresistive Manganites," *J. Magn. Magn. Mater.,* 1999, *200*(1), pp. 1-23.
3. Y. Moritomo, A. Asamitsu, H. Kuwahara, and Y. Tokura: "Giant Magnetoresistance of Manganese Oxides With a Layered Perovskite Structure," *Nature,* 1996, *380,* pp. 141-44.
4. A. Feltz, R. Kriegel, and W. Pölzl: "Sr$_7$Mn$_4$O$_{15}$ Ceramics for High Temperature NTC Thermistors," *J. Mater. Sci. Lett.,* 1999, *18,* pp. 1693-95.
5. T. Negas and R.S. Roth: "The System SrMnO$_{3-x}$," *J. Solid State Chem.,* 1970, *1,* pp. 409-18.
6. T. Negas: "The SrMnO$_{3-x}$-Mn$_3$O$_4$ System," *J. Solid State Chem.,* 1973, *7,* pp. 85-88.
7. K. Kuroda, S. Shinozaki, K. Uematsu, N. Mizutani, and M. Kato: "Phase Relation and Oxygen Deficiency of SrMnO$_{3-x}$," *Nippon Kagaku Kaishi,* 1977, *11,* pp. 1620-25 (in Japanese).
8. K. Kuroda, K. Shinozaki, K. Uematsu, N. Mizutani, and M. Kato: "Oxygen-Deficiency-Induced Polymorphs and Electrical Conductivity of SrMnO$_{3-x}$," *J. Am. Ceram. Soc.,* 1980, *63*(1), pp. 109-10.
9. N. Mizutani, A. Kitazawa, N. Ohkuma, and M. Kato: "Synthesis of Strontium-Manganese Double Oxides," *Kogyo Kagaki Zasshi,* 1970, *73*(6), pp. 1097-103 (in Japanese).
10. V. Caignaert, N. Nguyen, M. Hervieu, and B. Raveau: "Sr$_2$Mn$_2$O$_5$, an Oxygen-Deficient Perovskite with Mn(*III*) in Square Pyramidal Coordination," *Mater. Res. Bull.,* 1985, *20*(5), pp. 479-84.
11. T. Mori, K. Inoue, N. Kamegashira, Y. Yamaguchi, and K. Ohoyama: "Neutron Diffraction Study of Sr$_2$Mn$_2$O$_5$," *J. Alloys Compd.,* 2000, *296,* pp. 92-97.
12. O. Chmaissem, B. Dabrowski, S. Kolesnik, J. Mais, D.E. Brown, R. Kruk, P. Prior, B. Pyles, and J.D. Jorgensen: "Relationship between Structural Parameters and the Néel Temperature in Sr$_{1-x}$Ca$_x$MnO$_3$ ($0 \leq x \leq 1$) and Sr$_{1-y}$Ba$_y$MnO$_3$ ($y \leq 0.2$)," *Phys. Rev. B,* 2001, *64*(13), pp. 134412-13.
13. S.N. Ruddlesden and P. Popper: "The Compound Sr$_3$Ti$_2$O$_7$ and Its Structure," *Acta Crystallogr.,* 1958, *11,* pp. 54-55.
14. N. Mizutani, N. Ohkuma, A. Kitazawa, and M. Kato: "Modifications and Oxygen Deficiency of Strontium-Manganese Double Oxides, SrMnO$_{3-\delta}$ ($\delta = 0$-0.5)," *Kogyo Kagaki Zasshi,* 1970, *73*(6), pp. 1103-10 (in Japanese).
15. R. Kriegel, A. Feltz, L. Walz, A. Simon, and H.-J. Mattausch: "On the Compound Sr$_7$Mn$_4$O$_{15}$ and Its Relation to the Structures of Sr$_2$MnO$_4$ and α-SrMnO$_3$," *Z. Anorg. Allg. Chem.,* 1992, *617,* pp. 99-104 (in German).
16. K. Kuroda, N. Ishizawa, N. Mizutani, and M. Kato: "The Crystal Structure of α-SrMnO$_3$," *J. Solid State Chem.,* 1981, *38,* pp. 297-99.
17. P.D. Battle, T.C. Gibb, and C.W. Jones: "The Structural and Magnetic Properties of SrMnO$_3$: A Reinvestigation," *J. Solid State Chem.,* 1988, *74,* pp. 60-66.
18. R.S. Tichy and J.B. Goodenough: "Oxygen Permeation in Cubic SrMnO$_{3-\delta}$," *Solid State Sci.,* 2002, *4,* pp. 661-64.
19. D. Balz and K. Plieth: "The Structure of Potassium Nickel Fluoride, K$_2$NiF$_4$," *Z. Elektrochem.,* 1955, *59*(6), pp. 545-51 (in German).
20. K. Tezuka, M. Inamura, Y. Hinatsu, Y. Shimojo, and Y. Morii: "Crystal Structures and Magnetic Properties of Ca$_{2-x}$Sr$_x$O$_4$," *J. Solid State Chem.,* 1999, *145,* pp. 705-10.
21. J.F. Mitchell, J.E. Millburn, M. Medarde, S. Short, J.D. Jorgensen, and M.T. Fernández- Díaz, "Sr$_3$Mn$_2$O$_7$: Mn^{4+} Parent Compound of the $n = 2$ Layered CMR Manganites," *J. Solid State Chem.,* 1998, *141*(2), pp. 599-603.
22. J. Fabry, J. Hybler, Z. Jirak, K. Jurek, K. Maly, M. Nevriva, and V. Petricek: "Preparation and the Crystal Structure of a New Manganate, Sr$_4$Mn$_3$O$_{10}$." *J. Solid State Chem.,* 1988, *73,* pp. 520-23.
23. N. Floros, M. Hervieu, G. van Tendeloo, C. Michel, A. Maignan, and B. Raveau: "The Layered Manganate Sr$_{4-x}$Ba$_x$Mn$_3$O$_{10}$: Synthesis, Structural and Magnetic Properties," *Solid State Sci.,* 2000, *2,* pp. 1-9.
24. J.F. Vente, J.R. Plaisier, D.J.V. Ijdo, and K.V. Kamenev: "Preparation and Crystallographic Properties of Sr$_{7-x}$(Ca/Ba)$_x$Mn$_4$O$_{15}$," *Mater. Res. Bull.,* 2000, *35*(14-15), pp. 2437-44.
25. D. Risold, B. Hallstedt, and L.J. Gauckler: "The Strontium–Oxygen System." *Calphad,* 1996, *20*(3), pp. 353-61.
26. A.N. Grundy, B. Hallstedt, and L.J. Gauckler: "Assessment of the Mn-O System," *J. Phase Equilibria,* 2003, *24*(1), pp. 21-39.
27. M. Hillert: "The Compound Energy Formalism," *J. Alloys Compd., 320,* 161-176 (2001).
28. K. Frisk and M. Selleby: "The Compound Energy Formalism: Applications," *J. Alloys Compounds,* 2001, *320,* pp. 177-88.
29. M. Hillert, B. Jansson, B. Sundman, and J. Ågren: "A Two-Sublattice Model for Molten Solutions with Different Ten-

dency for Ionization," *Metall. Trans. A*, 1985, *16A*(2), pp. 261-66.

30. B. Sundman: "Modification of the Two-Sublattice Model for Liquids," *Calphad,* 1991, *15*(2), pp. 109-19.

31. J. Bouloux, J. Soubeyroux, G. Le Flem, and P. Hagenmuller: "Bidimensional Magnetic Properties of β-Sr_2MnO_4," *J. Solid State Chem.,* 1981, *38,* pp. 34-39.

32. J.F. Vente, K.V. Kamenev, and D.A. Sokolov: "Structural and Magnetic Properties of Layered $Sr_7Mn_4O_{15}$," *Phys. Rev. B,* 2001, *64*(21), pp. 214403-10.

33. B. Bochu, J. Chenavas, J.C. Joubert, and M. Marezio: "High Pressure Synthesis and Crystal Structure of a New Series of Perovskite-Like Compounds CMn_7O_{12} (C = Na, Ca, Cd, Sr, La, Nd)," *J. Solid State Chem.,* 1974, *11,* pp. 88-93.

34. G.H. Jonker and J.H. van Santen: "Ferromagnetic Compounds of Manganese with Perovskite Structure," *Physica,* 1950, *16*(3), pp. 337-49.

35. H. Yokokawa, N. Sakai, T. Kawada, and M. Dokiya: "Chemical Thermodynamic Considerations on Chemical Stability of $(La_{1-x}Sr_x)_yMnO_3$ Perovskite Air Electrode against Reaction with ZrO_2 Electrolyte in SOFC," *Denki Kagaku,* 1990, *58*(2), pp. 161-71 (in Japanese).

36. L. Rørmark, S. Stolen, K. Wiik, and T. Grande: "Enthalpies of Formation of $La_{1-x}A_xMnO_{3\pm\delta}$ (A = Ca and Sr) Measured by High-Temperature Solution Calorimetry," *J. Solid State Chem.,* 2002, *163,* pp. 186-93.

37. S. Tanasescu, N.D. Totir, and D.I. Marchidan: "Thermodynamic Properties of the $SrFeO_{2.5}$ and $SrMnO_{2.5}$ Brownmillerite-Like Compounds by Means of EMF-Measurements," *Solid State Ionics,* 2000, *134,* pp. 265-70.

38. M. Temkin: "Mixtures of Fused Salts as Ionic Solutions," *Acta Physicochim. URSS,* 1945, *20*(4), pp. 411-20.

39. A.T. Dinsdale: "SGTE Data for Pure Elements," *Calphad,* 1991, *15*(4), pp. 317-425.

40. B. Sundman, B. Jansson, and J.-O. Andersson: "The Thermo-Calc Databank System," *Calphad,* 1985, *9*(2), pp. 153-90.